Author Manuscript

Author Manuscript

Author Manuscript

Author Manuscript

HHS Public Access

Author manuscript

Radiology. Author manuscript; available in PMC 2016 March 01.

Published in final edited form as:

Radiology. 2015 March ; 274(3): 917–926. doi:10.1148/radiol.14141308.

Prospective Trial with Optical Molecular Imaging for Percutaneous Interventions in Focal Hepatic Lesions1

Rahul A. Sheth, MD, **Ronald S. Arellano, MD**, **Raul N. Uppot, MD**, **Anthony E. Samir, MD, MPH**, **Lipika Goyal, MD**, **Andrew X. Zhu, MD, PhD**, **Debra A. Gervais, MD**, and **Umar Mahmood, MD, PhD**

[1]Departments of Radiology (R.A.S., R.S.A., R.N.U., A.E.S., D.A.G., U.M.) and Hematology/Oncology (L.G., A.X.Z.), Massachusetts General Hospital, 149 13th St, Room 2301, Charlestown, MA 02129

Umar Mahmood: umahmood@mgh.harvard.edu

Abstract

Purpose—To demonstrate the clinical translation of optical molecular imaging (OMI) for the localization of focal hepatic lesions during percutaneous hepatic interventions.

Materials and Methods—Institutional review board approval was obtained for this prospective, single-center, HIPAA-compliant trial. Patients who were suspected of having hepatocellular carcinoma or liver metastases from colorectal cancer and were scheduled for percutaneous liver biopsy or thermal ablation were eligible for this study. Patients (n = 5) received 0.5 mg per kilogram of body weight of indocyanine green (ICG) intravenously 24 hours prior to their scheduled procedure in this study. Intraprocedurally, a handheld device composed of an endoscope that fits coaxially through a standard 17-gauge introducer needle was advanced into the liver, and real-time measurements of ICG fluorescence were obtained. A point-of-care fluorescence imaging system was used to image ICG fluorescence in biopsy samples. Target-to-background ratios (TBRs) were calculated by dividing the mean fluorescence intensity in the lesion by the mean fluorescence intensity in the adjacent liver parenchyma. The reference standard for determination of proper needle positioning in patients undergoing biopsy was final pathologic analysis of biopsy specimens or follow-up imaging.

© RSNA, 2014

Correspondence to: Umar Mahmood, umahmood@mgh.harvard.edu.

Online supplemental material is available for this article.

Author contributions:

Guarantors of integrity of entire study, R.A.S., R.N.U., A.X.Z., U.M.; study concepts/study design or data acquisition or data analysis/interpretation, all authors; manuscript drafting or manuscript revision for important intellectual content, all authors; approval of final version of submitted manuscript, all authors; agrees to ensure any questions related to the work are appropriately resolved, all authors; literature research, R.A.S., U.M.; clinical studies, R.A.S., R.S.A., R.N.U., L.G., A.X.Z.; statistical analysis, R.A.S.; and manuscript editing, all authors

Disclosures of Conflicts of Interest: R.A.S. disclosed no relevant relationships. **R.S.A.** disclosed no relevant relationships. **R.N.U.** disclosed no relevant relationships. **A.E.S.** Financial activities related to the present article: disclosed no relevant relationships. Financial activities not related to the present article: disclosed no relevant relationships. Other relationships: has patents pending for optical device for fluorescent pathology and optical fluorescent needle. **L.G.** disclosed no relevant relationships. **A.X.Z.** disclosed no relevant relationships. **D.A.G.** Financial activities related to the present article: disclosed no relevant relationships. Financial activities not related to the present article: disclosed no relevant relationships. Other relationships: received a Covidien/Valleylab research grant. **U.M.** disclosed no relevant relationships.

Author Manuscript Author Manuscript Author Manuscript Author Manuscript

Results—Intraprocedural OMI was successfully performed in six lesions (two lesions in patient 3) in five patients. The median size of the targeted lesions was 16 mm (range, 10–21 mm). Four of five biopsies (80%) yielded an accurate pathologic diagnosis, and one biopsy specimen showed benign liver parenchyma; both ablated lesions showed no residual disease 1 month after the procedure. The median overall added procedure time to perform OMI was 2 minutes. ICG was found to localize with TBRs greater than 2.0 (median, 7.9; range, 2.4–13.4) in all target lesions. No trial-related adverse events were reported.

Conclusion—The clinical translation of OMI to percutaneous hepatic interventions was demonstrated.

Percutaneous interventions on focal hepatic lesions are among the most commonly performed procedures in interventional radiology. Biopsies of focal hepatic lesions are necessary to establish tissue diagnosis of primary or metastatic hepatic malignancy, as well as to perform genotype analysis in this era of molecularly targeted drug therapies. Thermal ablative procedures such as microwave or radiofrequency ablation likewise are important local-regional therapies for patients with small focal hepatic lesions.

As cross-sectional diagnostic imaging techniques have improved during the past 2 decades, the ability to detect focal hepatic lesions earlier in the disease process has improved. Consequently, the rate of percutaneous interventions in small focal hepatic lesions less than 30 mm in size has increased (1). Small hepatic lesions, however, can pose several challenges for the interventionalist. For example, some lesions may be identified with magnetic resonance (MR) imaging, but most procedures are performed with computed tomography (CT) or ultrasonography (US) guidance, and the lesion may be “invisible” at intraprocedural imaging. For CT-guided procedures, an important limitation is the beam-hardening artifact caused by the biopsy needle.

Operator confidence in accurate needle placement with the use of conventional CT or US guidance for biopsies and ablations decreases as target lesions decrease in size (2). There exists a clinical need for a real-time, accurate method for confirming proper needle position during percutaneous hepatic interventions to complement existing image guidance technologies. Optical molecular imaging (OMI) with exogenously administered organic fluorochromes is a real-time imaging discipline that holds promise for minimally invasive procedural guidance. Indocyanine green (ICG) is a clinically approved OMI agent that fluoresces in the near-infrared spectrum and has been shown during liver resection surgery to localize with high sensitivity and target-to-background ratios (TBRs) to hepatocellular carcinomas (HCCs) and intrahepatic colorectal cancer (CRC) metastases in human clinical trials (3–9). The potential for performing minimally invasive OMI of ICG localization to focal hepatic lesions has been demonstrated in the preclinical setting (10). The purpose of this study was to demonstrate the clinical translation of OMI for the localization of focal hepatic lesions during percutaneous hepatic interventions.

Author Manuscript Author Manuscript Author Manuscript Author Manuscript

Materials and Methods

Study Design

Institutional review board approval was obtained for this prospective, single-center, Health Insurance Portability and Accountability Act–compliant trial. The eligibility and exclusion criteria are summarized in Figure 1. This report presents the initial cohort of subjects enrolled between January 1, 2014, and June 1, 2014. All participants (n = 5) provided written informed consent. ICG was prepared for intravenous injection by the institutional research pharmacy at a dose of 0.5 mg per kilogram of body weight, with a maximum dose of 40 mg. ICG was administered as a bolus 1 day prior to the patient's scheduled procedure.

On the day of the procedure (approximately 24 hours after ICG injection), the patients were positioned, prepared, and draped, as would be routinely performed for a conventional percutaneous hepatic intervention. The biopsy or ablation introducer needle was then advanced toward the target lesion by using standard US or CT guidance. When the introducer needle was positioned in the liver but not in the target lesion, a measurement of ICG fluorescence of liver tissue was performed by removing the inner stylet of the introducer needle and advancing the handheld OMI device coaxially through the introducer; this measurement established the ICG background fluorescence. The OMI device was then removed, the stylet was replaced, and the introducer was positioned in the target lesion by using CT or US guidance. The interventional radiologist performing the procedure was permitted to perform any maneuvers necessary to facilitate proper needle placement and minimize complications, including administering intravenous iodinated contrast material or repositioning the patient. Once the needle was positioned in the target lesion, the handheld device was once again passed coaxially through the introducer needle, and a second measurement of ICG fluorescence was acquired; these data provided the "target" fluorescence intensity. Biopsy specimens were then obtained, and the fluorescence intensity of the specimens was imaged by using the point-of-care imaging system, which was located within the procedure room. For patients undergoing thermal ablation, the microwave antenna was advanced through the introducer needle, and thermal ablation was performed. The additional procedure time required for performing OMI with the handheld device was measured by one author (R.A.S.) by using a stopwatch.

The reference standard for determination of proper needle positioning in patients undergoing biopsy was final pathologic analysis of biopsy specimens. For patients undergoing thermal ablation without biopsy, the reference standard for determination of on-target treatment was the 1-month postprocedural imaging examination to evaluate the location of the ablation zone relative to the targeted lesion; response to therapy was assessed by using modified Response Evaluation Criteria in Solid Tumors (11) criteria. All biopsy and ablation procedures were performed by three board-certified attending radiologists who had subspecialty experience in abdominal interventions (R.N.U., with 11 years of experience; R.S.A., with 16 years of experience; and A.E.S., with 11 years of experience). Fluorescence imaging with the handheld device and point-of-care system was performed by one author (R.A.S., with 10 years of experience in OMI).

Author Manuscript Author Manuscript Author Manuscript Author Manuscript

In addition to our institution's standard follow-up protocols, patients were contacted via telephone on postprocedural days 1 and 7 to assess for any adverse events.

Point-of-Care OMI System

The hardware and software components of the point-of-care epifluorescence OMI system (Fig 2, *A*) are based on the design of multiple prior imaging systems (12–14). Fluorescence excitation light is provided by a 450-mW, 785-nm laser (Edmund Optics, Barrington, NJ). Emitted fluorescent light is collected by a close focus video zoom lens (Edmund Optics) and filtered by a band-pass filter (FF01-832/37-25; Semrock, Rochester, NY) to exclude reflected excitation laser light. The filtered fluorescent light is then imaged with a near-infrared–optimized high-temporal- and high-spatial-resolution camera (Manta; Allied Vision Technologies, Stadtroda, Germany). The hardware is fixed in position with a rigid frame. The point-of-care imaging system has dimensions and optical features that are summarized in Table 1.

Handheld OMI System

The handheld OMI system was constructed as previously described (10). Briefly, the endoscopic portion of the handheld OMI system consisted of a clinically approved pediatric cystoscope (Karl Storz, Tuttlingen, Germany) that could pass coaxially through the introducer of a standard 17-gauge core biopsy system (Temno; CareFusion, San Diego, Calif) or a 16-gauge microwave ablation system (Amica; HS Medical, Boca Raton, Fla). The imaging endoscope was the only component that was in contact with the patient, and it was sterilized prior to each patient's examination. The remainder of the handheld device was wrapped in a sterile plastic sleeve. The eyepiece of the endoscope was attached to a near-infrared–optimized high-temporal- and high-spatial-resolution camera (Manta; Allied Vision Technologies), and the light output was filtered through an 832-nm band-pass filter (FF01–832/37–25; Semrock). The illumination port of the endoscope was attached with fiberoptic cable to a 450-mW, 785-nm laser excitation source (Edmund Optics). Real-time image display (Movie 1 [online]) and camera functions are controlled from a laptop by using a custom-designed software program developed by one of the authors (R.A.S.).

Image Analysis

Image analysis was performed by one author (R.A.S.). Analysis of the fluorescence data was performed by drawing regions of interest within the circular projected image using a standard software package and measuring the mean pixel intensity (ImageJ; National Institutes of Health, Bethesda, Md). Fluorescence intensity was normalized by dividing the mean pixel intensity by the exposure time of the image to arrive at a counts per millisecond value that could be compared across images with varying exposure times. TBRs were calculated by dividing the mean fluorescence intensity within the lesion by the mean fluorescence intensity within the adjacent liver parenchyma. Mean fluorescence intensities for liver, biopsy target lesions, and ablation target lesions for all patients were plotted by using software (GraphPad Prism, La Jolla, Calif).

Author Manuscript Author Manuscript Author Manuscript Author Manuscript

Statistical Analysis

Statistical analysis was performed by one author (R.A.S.). Significance for differences in ICG fluorescence intensity in normal liver versus focal lesions was calculated by using Wilcoxon nonparametric analysis with a standard statistical software package (R; R Foundation for Statistical Computing, Vienna, Austria); an α value of less than .05 was used as the threshold for a significant difference.

Results

Patient Population

The demographics for the trial participants are summarized in Table 2. The patients were referred to the Interventional Radiology Department at our institution for a broad range of indications. All participants were men (mean age, 64 years; range, 55–73 years), and most (three of five) had a history of Child-Pugh class A cirrhosis. Percutaneous biopsies were performed in all participants, and two participants additionally underwent thermal ablation, either to an additional lesion (patient 3) or to the same lesion for which the patient underwent biopsy (patient 4). The median size of the targeted lesions was 16 mm (range, 10–21 mm). Intravenous iodinated contrast material was administered to facilitate visualization of the target lesions for patients 3 and 4. Four of five biopsies (80%) yielded an accurate pathologic diagnosis, and one biopsy specimen showed benign liver parenchyma.

Intraprocedural ICG Fluorescence

Intraprocedural imaging of ICG fluorescence intensity at the tip of a standard introducer needle and within core biopsy specimens was feasible and added less than 5 minutes (median, 2 minutes) of procedure time in all patients (Table 3). ICG was found to localize with TBRs greater than 2.0 (range, 2.4–13.4; median, 7.9) in all target lesions including primary HCC, metastatic CRC, and a nonneoplastic granulomatous process. The difference between ICG fluorescence intensity between normal liver and focal hepatic lesions across the study cohort approached significance ($P = .06$). No trial-specific adverse events were observed up to 7 days following the procedures.

Examination Results in Patients

Below are the results of examinations in all five patients

Patient 1—Patient 1 was a 55-year-old man with an unremarkable medical history who underwent CT of the abdomen and pelvis for chronic diffuse abdominal pain that revealed multiple focal hypoattenuating lesions measuring approximately 10 mm in the liver; a fluorine 18 fluorodeoxyglucose positron emission tomography examination revealed the lesions to be fluorine 18 fluorodeoxyglucose–avid, raising the suspicion for occult malignancy, including CRC with hepatic metastases. Percutaneous biopsy of a focal hepatic lesion at an outside hospital was nondiagnostic (normal hepatocytes only), and the patient was subsequently referred to our institution for repeat biopsy.

The patient's biopsy was performed with US guidance (Fig 3). A subtle, approximately 13-mm hyperechoic lesion in the right hepatic lobe was targeted for biopsy. Fluorescence

Author Manuscript Author Manuscript Author Manuscript Author Manuscript

intensity measurements acquired with the handheld OMI device through the biopsy introducer needle revealed a TBR of 8.9. Similarly, surface reflectance fluorescence imaging of core samples using the point-of-care OMI system revealed focal areas of increased ICG localization. Histologic evaluation of the core specimens was notable for no evidence of malignancy but rather intrahepatic granulomas. The patient was subsequently referred for further diagnostic workup of both infectious and noninfectious granulomatous diseases.

Patient 2—Patient 2 was a 67-yearold man with HCV cirrhosis who had a 21-mm focal hepatic lesion in segment VIII on a screening MR image. Given that the patient had a history of renal cell carcinoma previously treated with thermal ablation, biopsy was requested to definitively characterize the hepatic lesion as a primary HCC versus a renal cell carcinoma metastasis.

Biopsy was performed with US guidance (Fig 4). The TBR, as measured by using the handheld OMI device, was 6.8, and fluorescence imaging of a core biopsy sample revealed intensely fluorescent tissue. Findings at histologic assessment of the biopsy specimens were consistent with high-grade HCC.

Patient 3—Patient 3 was a 62-year-old man with HCV and alcoholic cirrhosis who presented for biopsy of a peripherally enhancing, centrally necrotic 18-mm mass in segment VII and thermal ablation of a 15-mm biopsy-proven HCC in segment V. The biopsy and ablation were performed in a single setting and with general anesthesia, given the patient's comorbidities.

Intravenous contrast material (iopamidol, Isovue-370; Bracco, Monroe Township, NJ), 80 mL, was administered, followed by arterial (30-second delay) and portal venous (70-second delay) CT imaging during the CT-guided procedure to confirm adequacy of needle placement. Hydrodissection with 750 mL of 0.9% normal saline was first performed to displace the liver margin from the abdominal wall, given the peripheral location of the ablation target. Biopsy of the lesion in segment VII was then pursued; TBR of ICG fluorescence using the handheld OMI device was 2.4. An introducer needle was next advanced into the ablation target, and fluorescence imaging using the handheld OMI device revealed a TBR of 13.4 for this grade 1 HCC in which a biopsy was previously performed. The microwave antenna was then advanced through the introducer, and a single microwave ablation was performed.

Pathologic findings of the biopsy samples from the segment VII lesion were consistent with a high-grade, necrotic HCC. Subsequent liver MR imaging examinations in the 3 months following the patient's procedure demonstrated complete response to ablation of the low-grade HCC but interval significant growth and macrovascular invasion of the high-grade HCC in which a biopsy had been performed (Fig 5).

Patient 4—Patient 4 was a 73-year-old man with cirrhosis due to hemochromatosis who had a 10-mm arterially enhancing lesion in segment VII on a screening MR image. The patient had a remote history of low-grade CRC treated with curative surgical resection; the differential diagnosis of this lesion was HCC versus CRC metastasis. Given the remoteness

Author Manuscript Author Manuscript Author Manuscript Author Manuscript

of the CRC diagnosis, the high likelihood of HCC, and the necessity for general anesthesia for any hepatic intervention, the decision was made to pursue focal liver biopsy followed by thermal ablation of the target lesion within one procedure setting.

A single introducer was advanced with CT guidance to the target lesion. Intravenous contrast medium (iopamidol, Isovue-370; Bracco), 80 mL, was administered, followed by arterial (30-second delay) and portal venous (70-second delay) phase CT imaging to facilitate lesion identification. When the introducer was positioned within the target, as best determined with contrast-enhanced CT, the handheld OMI device was inserted through the introducer. ICG fluorescence in this location was similar in intensity to background liver fluorescence for this patient. By torqueing the hub of the introducer so that the tip was angled superiorly, a focal bright spot of ICG fluorescence came into view (Movie 2 [online]). However, given that the introducer appeared to be properly positioned within the target lesion by using standard-of-care procedural imaging, the introducer was not repositioned, and biopsy samples were acquired. After the biopsy, a microwave antenna was advanced through the same introducer, and two overlapping thermal ablations were performed.

Histologic analysis of the biopsy specimens revealed benign liver parenchyma only. The procedural imaging results were then retrospectively reviewed by the radiologist who performed the biopsy and ablation; it was concluded that the biopsy needle had been approximately 5 mm inferior to the target lesion. At 1-month follow-up, contrast-enhanced MR imaging revealed that the target lesion had been successfully treated with the two overlapping thermal ablations.

Patient 5—Patient 5 was a 66-year-old man who had a synchronous stage IIIB sigmoid adenocarcinoma and stage IIIB right colonic adenocarcinoma, as well as a focal hepatic lesion measuring 17 mm in segment VII that was suspected of being a metastasis. The patient first underwent partial colectomy and then was referred for tissue confirmation of hepatic metastatic disease.

Percutaneous focal liver biopsy was performed with nonenhanced CT guidance. The TBR, as measured by using the handheld OMI device, was 10.8, and in one of the core specimens that contained both tumor and a small quantity of normal liver, the point-of-care OMI system revealed ICG fluorescence localized to the malignant tissue only (Fig 6). Histologic analysis confirmed the diagnosis of metastatic CRC.

Comparison of ICG Fluorescence Intensity Measurements

Figure 7 includes a plot of normalized ICG fluorescence intensity measurements for background, biopsy lesions, and ablation targets in all five patients.

Discussion

We have demonstrated the feasibility of OMI assistance for percutaneous interventions. We applied a handheld OMI device that complements existing interventional needles and imaging technologies to provide intraprocedural confirmation of needle tip position during

Author Manuscript Author Manuscript Author Manuscript Author Manuscript

percutaneous liver biopsies and ablations, with minimal additional time; we also developed and evaluated a point-of-care OMI system to measure ICG localization to core biopsy specimens. We have shown that ICG imaging using these systems is a robust adjunct to conventional image guidance for patients undergoing biopsy of primary HCC, hepatic CRC metastasis, and nonneoplastic inflammatory processes, as well as thermal ablations.

ICG is an OMI agent that has been clinically available for decades but has only relatively recently been shown to localize to focal hepatic lesions up to 2 weeks after injection (4,5,8,10). While we measured TBRs greater than 2.0 for all biopsy lesions positive for disease, there was variability in fluorescence intensity of the background hepatic parenchyma across the study cohort. There are two possible explanations for this finding. First, variations in background hepatic ICG fluorescence may reflect variations in hepatic function among the patients, which in turn would affect the rate of ICG clearance from the liver. While all of the existing data on ICG imaging of hepatic lesions have been acquired from patients undergoing surgery who have relatively preserved liver function, the patient populations undergoing biopsy and ablation have, in general, relatively worse liver function. Second, it is possible that there was a false elevation of background hepatic fluorescence intensity caused by “shine-through” from the underlying tumor. That is, while we attempted to measure background fluorescence images in nonmalignant tissue well removed from the target lesion, it is possible that the intense fluorescence of the lesion, albeit attenuated by the interposed tissue, contributed to the background signal measurement. More data are required to establish quantitative thresholds for benign versus pathologic fluorescence intensities.

Two discrete mechanisms for tumor localization have been proposed and partially substantiated in human clinical trials. ICG uptake into normal hepatocytes is mediated by two principal sinusoidal surface transporters, Na^+/taurocholate cotransporting polypeptide and organic anion-transporting polypeptide 8. In well-differentiated HCC, expression of Na^+/taurocholate cotransporting polypeptide and organic anion-transporting polypeptide 8 is maintained (4), and so ICG uptake into the malignant cells is preserved. However, because of impaired biliary excretion, ICG is retained within the cell, resulting in a diffuse pattern of ICG enhancement throughout the tumor. Alternatively, for poorly differentiated HCC and intrahepatic CRC metastases, there is limited intracellular uptake of ICG because of downregulation of Na^+/taurocholate cotransporting polypeptide and organic anion-transporting polypeptide 8 (4). Instead, these lesions demonstrate a peripheral, rimlike pattern of ICG enhancement. The cells demonstrating ICG uptake in these tumors are probably not cancer cells at all, but rather immature hepatocytes that comprise the inflammatory microenvironmental response to intrahepatic tumors (8). These immature hepatocytes may behave in a way similar to the way HCC cells behave with respect to ICG retention insofar as they maintain the capability to take up ICG but lack the capability to excrete ICG. It has also been proposed that ICG accumulates within bile ducts that are physically obstructed by mass effect from the metastases, resulting in the peripheral, rimlike accumulation of ICG around CRC metastases.

There is an expanding role for fluorescence imaging guidance systems in clinical medicine. Stereotactic fluorescence microscopes have become increasingly common in neurosurgery for blood vessel visualization (15), as well as tumor margin clarification (16). Handheld

Author Manuscript Author Manuscript Author Manuscript Author Manuscript

fluorescence imaging devices for open (5), as well as laparoscopic (D-Light system; Karl Storz, Tuttlingen, Germany), abdominal surgery are commercially available. Moreover, confocal microendoscopy can be performed through the working channel of clinical endoscopes for microscopic resolution fluorescence imaging (17,18).

In addition to new fluorescence imaging systems, clinical trial evaluation of multiple fluorescent pharmaceuticals has been successfully completed or is currently under way. For example, fluorescence imaging of 5-aminolevulinic acid localization to malignant gliomas allows for more complete surgical resections and improves progression-free survival (16). Also, protease-activatable OMI agents have been shown to serve as highly effective beacons for malignancy and cardiovascular disease in the preclinical setting, and the human translation of one such agent is currently being investigated (ClinicalTrials.gov identifier NCT01626066).

Our data indicate that ICG is a sensitive marker for intrahepatic pathologic findings but is not specific to any one particular disease process, an ideal behavior for an OMI agent in interventional radiology, as the nature of focal hepatic lesions undergoing percutaneous biopsy is often not known a priori. Confidence in the accuracy of a needle position during percutaneous hepatic interventions is essential. The very need for improved tools was illustrated in our trial, wherein the biopsy in patient 4 was performed by using standard imaging guidance and the result was presumed to be false-negative. Moreover, because the lesion was subsequently treated with thermal ablation, a repeat biopsy could not be performed. This case highlights the very narrow margin for error for percutaneous biopsies. As the clinical experience with interventional OMI improves, and as the confidence in OMI as a molecular beacon for pathologic processes increases, OMI could be used as a real-time guidance tool for repositioning biopsy needles in the crucial final 10 mm of distance to the target lesion. And, while in our trial the ICG data were not used to alter intraprocedural decision making, it is possible that intense ICG fluorescence measured at the margin of an ablation zone could serve as an indicator for residual malignancy and motivate additional overlapping ablations.

There were several limitations to our study. While we were able to demonstrate high TBRs for ICG localization to focal hepatic lesions, there was a broad range in the TBRs. This finding is probably a reflection of the broad range of pathologic findings that were imaged and is corroborated by the surgical literature in which low-grade HCCs have been shown to fluoresce homogeneously, while high-grade HCCs and metastases demonstrate a thin rim of ICG enhancement (4,8). Moreover, a large clinical trial in which patients are randomized to groups of procedures with or without OMI guidance is necessary to show that intraprocedural OMI can improve the accuracy of biopsies and the complete response rate for thermal ablations. Another important limitation is the depth of tissue penetration of near-infrared photons within the liver, which is on the order of approximately 1 cm. Given the high degree of signal attenuation, we performed measurements of lesion fluorescence intensity with the handheld device tip well seated within the lesions. However, it is conceivable that improvements in device technology will allow for true image guidance, with fluorescence imaging providing a beacon to guide needle placement.

Author Manuscript Author Manuscript Author Manuscript Author Manuscript

OMI is a safe, accurate adjunctive imaging modality that can be performed during percutaneous hepatic interventions with existing clinical equipment and with minimal added procedure time. This technology can be used to potentially provide real-time guidance to improve procedural accuracy and operator confidence during biopsies and thermal ablations. While ICG is an effective OMI agent for hepatic interventions, as newer OMI agents currently in clinical trials are approved for human use, a broadening in the paradigm of OMI guidance and characterization for a wide range of organs and disease processes is anticipated.

Supplementary Material

Refer to Web version on PubMed Central for supplementary material.

Acknowledgments

R.A.S. supported by 2013 Cook Medical Cesare Gianturco/RSNA Research Resident Grant RR1348 and a Society for Interventional Radiology Foundation research resident grant.

Funding:

This research was supported by the National Institutes of Health (grants U01CA084301 and P50CA127003).

Abbreviations

CRC	colorectal cancer
HCC	hepatocellular carcinoma
HCV	hepatitis C virus
ICG	indocyanine green
OMI	optical molecular imaging
TBR	target-to-background ratio

References

1. Ma X, Arellano RS, Gervais DA, Hahn PF, Mueller PR, Sahani DV. Success of image-guided biopsy for small (≤ 3 cm) focal liver lesions in cirrhotic and noncirrhotic individuals. J Vasc Interv Radiol. 2010; 21(10):1539–1547. quiz 1547. [PubMed: 20801683]
2. Stattaus J, Kuehl H, Ladd S, et al. CT-guided biopsy of small liver lesions: visibility, artifacts, and corresponding diagnostic accuracy. Cardiovasc Intervent Radiol. 2007; 30(5):928–935. [PubMed: 17546404]
3. Kokudo N, Ishizawa T. Clinical application of fluorescence imaging of liver cancer using indocyanine green. Liver Cancer. 2012; 1(1):15–21. [PubMed: 24159568]
4. Ishizawa T, Masuda K, Urano Y, et al. Mechanistic background and clinical applications of indocyanine green fluorescence imaging of hepatocellular carcinoma. Ann Surg Oncol. 2014; 21(2): 440–448. [PubMed: 24254203]
5. Ishizawa T, Fukushima N, Shibahara J, et al. Real-time identification of liver cancers by using indocyanine green fluorescent imaging. Cancer. 2009; 115(11):2491–2504. [PubMed: 19326450]
6. Morita Y, Sakaguchi T, Unno N, et al. Detection of hepatocellular carcinomas with near-infrared fluorescence imaging using indocyanine green: its usefulness and limitation. Int J Clin Oncol. 2013; 18(2):232–241. [PubMed: 22200990]

Author Manuscript Author Manuscript Author Manuscript Author Manuscript

7. Schaafsma BE, Mieog JSD, Hutteman M, et al. The clinical use of indocyanine green as a near-infrared fluorescent contrast agent for image-guided oncologic surgery. J Surg Oncol. 2011; 104(3): 323–332. [PubMed: 21495033]
8. van der Vorst JR, Schaafsma BE, Hutteman M, et al. Near-infrared fluorescence-guided resection of colorectal liver metastases. Cancer. 2013; 119(18):3411–3418. [PubMed: 23794086]
9. van der Vorst JR, Hutteman M, Mieog JSD, et al. Near-infrared fluorescence imaging of liver metastases in rats using indocyanine green. J Surg Res. 2012; 174(2):266–271. [PubMed: 21396660]
10. Sheth RA, Heidari P, Esfahani SA, Wood BJ, Mahmood U. Interventional optical molecular imaging guidance during percutaneous biopsy. Radiology. 2014; 271(3):770–777. [PubMed: 24520946]
11. Lencioni R, Llovet JM. Modified RECIST (mRECIST) assessment for hepatocellular carcinoma. Semin Liver Dis. 2010; 30(1):52–60. [PubMed: 20175033]
12. Sheth RA, Tam JM, Maricevich MA, Josephson L, Mahmood U. Quantitative endovascular fluorescence-based molecular imaging through blood of arterial wall inflammation. Radiology. 2009; 251(3):813–821. [PubMed: 19474377]
13. Upadhyay R, Sheth RA, Weissleder R, Mahmood U. Quantitative real-time catheter-based fluorescence molecular imaging in mice. Radiology. 2007; 245(2):523–531. [PubMed: 17940307]
14. Sheth RA, Upadhyay R, Weissleder R, Mahmood U. Real-time multichannel imaging framework for endoscopy, catheters, and fixed geometry intraoperative systems. Mol Imaging. 2007; 6(3): 147–155. [PubMed: 17532881]
15. Raabe A, Beck J, Gerlach R, Zimmermann M, Seifert V. Near-infrared indocyanine green video angiography: a new method for intraoperative assessment of vascular flow. Neurosurgery. 2003; 52(1):132–139. discussion 139. [PubMed: 12493110]
16. Stummer W, Pichlmeier U, Meinel T, et al. Fluorescence-guided surgery with 5-aminolevulinic acid for resection of malignant glioma: a randomised controlled multicentre phase III trial. Lancet Oncol. 2006; 7(5):392–401. [PubMed: 16648043]
17. Hsiung PL, Hardy J, Friedland S, et al. Detection of colonic dysplasia in vivo using a targeted heptapeptide and confocal microendoscopy. Nat Med. 2008; 14(4):454–458. [PubMed: 18345013]
18. Goetz M, Ziebart A, Foersch S, et al. In vivo molecular imaging of colorectal cancer with confocal endomicroscopy by targeting epidermal growth factor receptor. Gastroenterology. 2010; 138(2): 435–446. [PubMed: 19852961]

Author Manuscript Author Manuscript Author Manuscript Author Manuscript

Advance in Knowledge

- Indocyanine green, a Food and Drug Administration–approved near-infrared fluorochrome, localizes to intrahepatic lesions with high target-to-background ratios; here, we present human measurements of this accumulation with a percutaneous, handheld optical molecular imaging (OMI) system, representing the clinical application of OMI in the interventional radiology setting.

Author Manuscript Author Manuscript Author Manuscript Author Manuscript

Implication for Patient Care

- OMI localization of focal hepatic lesions during percutaneous hepatic interventions is feasible and may help improve accuracy and reduce false-negative results of biopsies.

Author Manuscript Author Manuscript Author Manuscript Author Manuscript

Eligibility criteria
Patients with imaging findings suspicious for HCC or hepatic CRC metastasis, for whom image-guided percutaneous biopsy is planned
Patients with HCC, as characterized by prior biopsy or diagnostic imaging findings, for whom thermal ablation is planned
Age > 18 years
Life expectancy greater than 6 months
Platelets > 50 000/μL
Exclusion criteria
Patients with documented allergy to iodine or iodine-containing compounds
Patients with documented allergy to sulfur-containing compounds
History of adverse reactions to percutaneous procedures or sedatives for endoscopy, thermal ablation, or biopsy
Pregnancy

Figure 1.
Chart shows eligibility and exclusion criteria.

Author Manuscript Author Manuscript Author Manuscript Author Manuscript

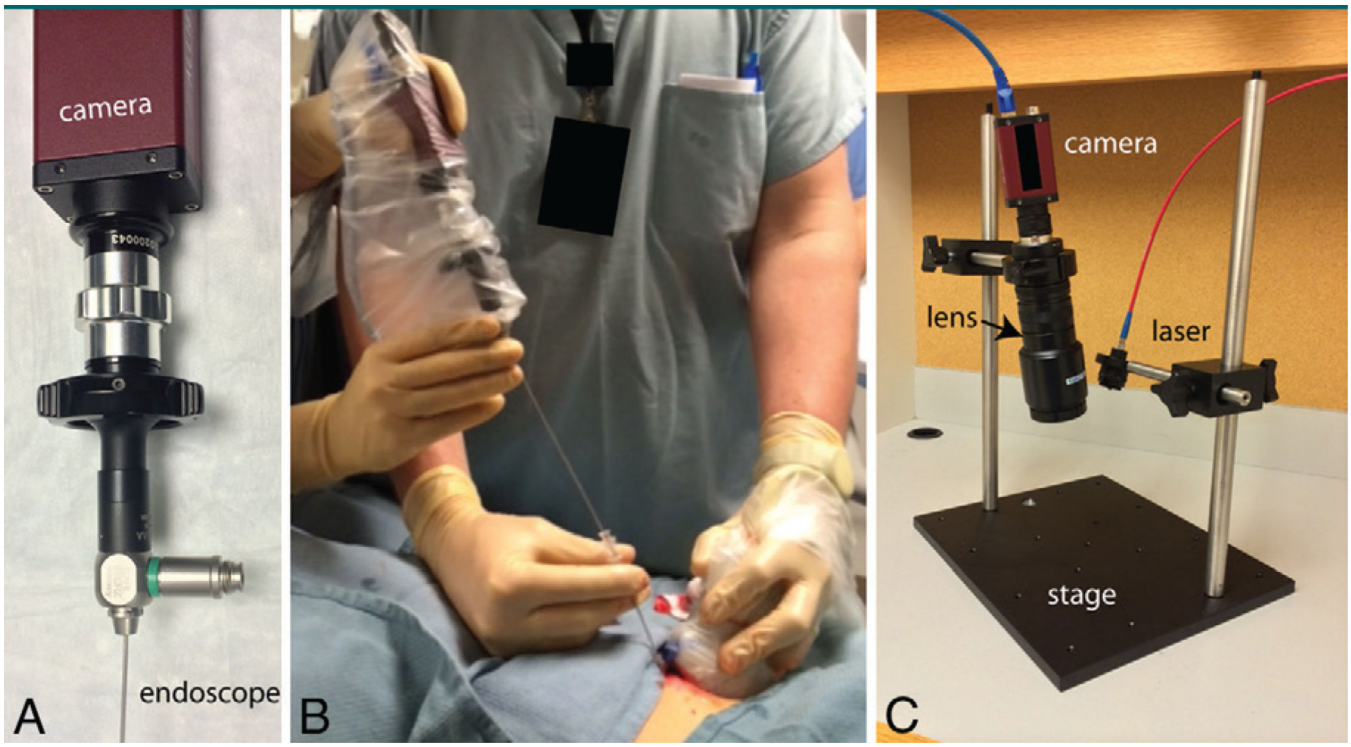

Figure 2.

Photographs of the OMI devices used in the clinical trial. *A*, Handheld OMI device consists of a miniature endoscope coupled to a high-temporal- and high-spatial-resolution 12-bit camera. *B*, Handheld device advanced through a standard 17-gauge introducer needle during US-guided percutaneous focal liver biopsy to perform real-time measurements of ICG localization. *C*, Point-of-care OMI system for acquisition of high-temporal- and high-spatial-resolution ICG fluorescence images of biopsy cores during biopsy procedures.

Author Manuscript Author Manuscript Author Manuscript Author Manuscript

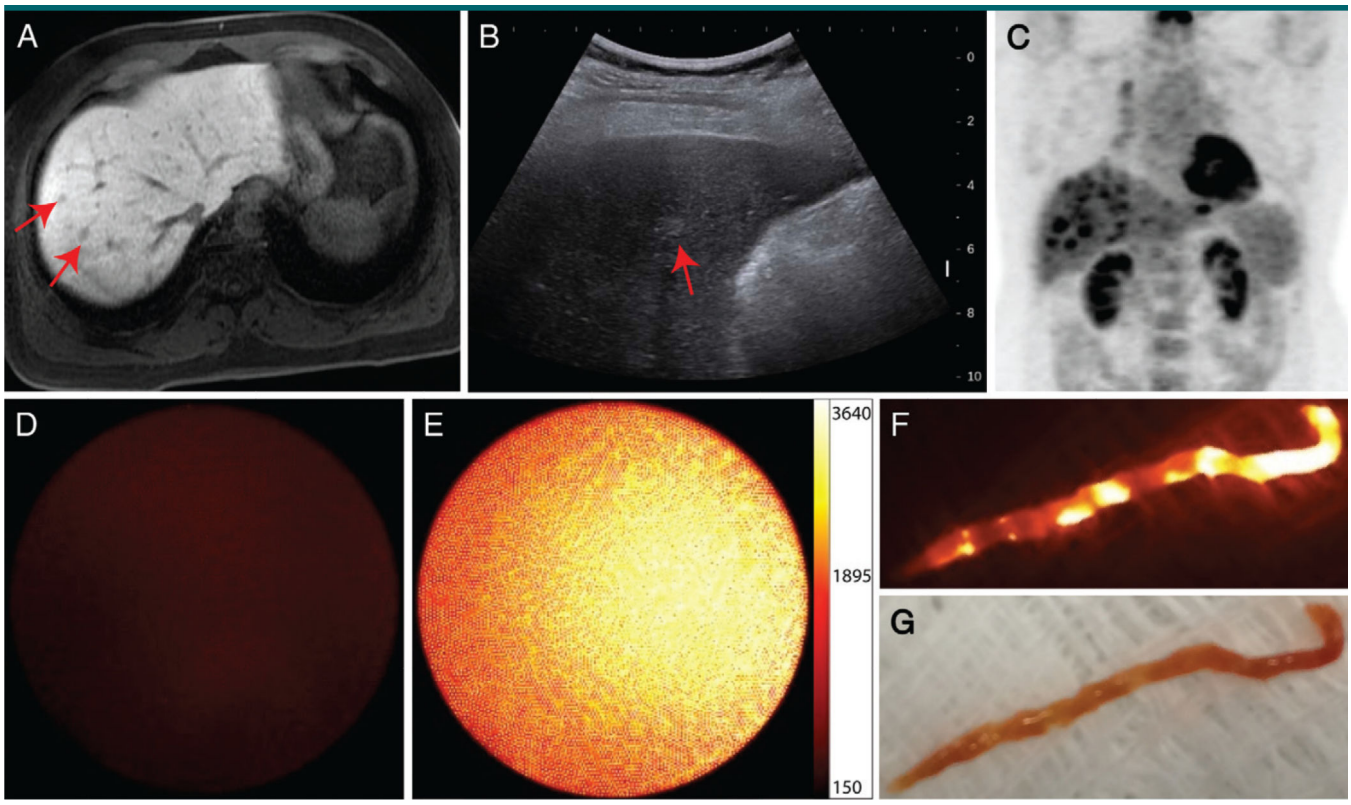

Figure 3.

Subcentimeter focal hepatic lesions on, *A*, T1-weighted gadoxetic acid–enhanced MR image obtained in the hepatobiliary phase and, *B*, US image. *C*, Fluorine 18 fluorodeoxyglucose positron emission tomographic scan shows fluorine 18 fluorodeoxyglucose–avid lesion (arrows on *A* and *B*) that was suspected of being a malignancy in a 55-year-old man (patient 1). At a prior outside hospital, the liver biopsy result was nondiagnostic, and the patient was referred to our institution for further management. Intraprocedural optical molecular images confirmed the accuracy of the biopsy needle placement, by measuring increased fluorescence, *E*, in the target lesion relative to, *D*, normal liver. Optical molecular images of core biopsy specimen show visualized areas of, *F*, focally increased ICG localization, *G*, in the core specimen (photograph). Final pathologic analysis of the core specimens revealed a nonneoplastic granulomatous process, with subsequent results of clinical and serologic evaluations most suggestive of sarcoidosis.

Author Manuscript
Author Manuscript
Author Manuscript
Author Manuscript

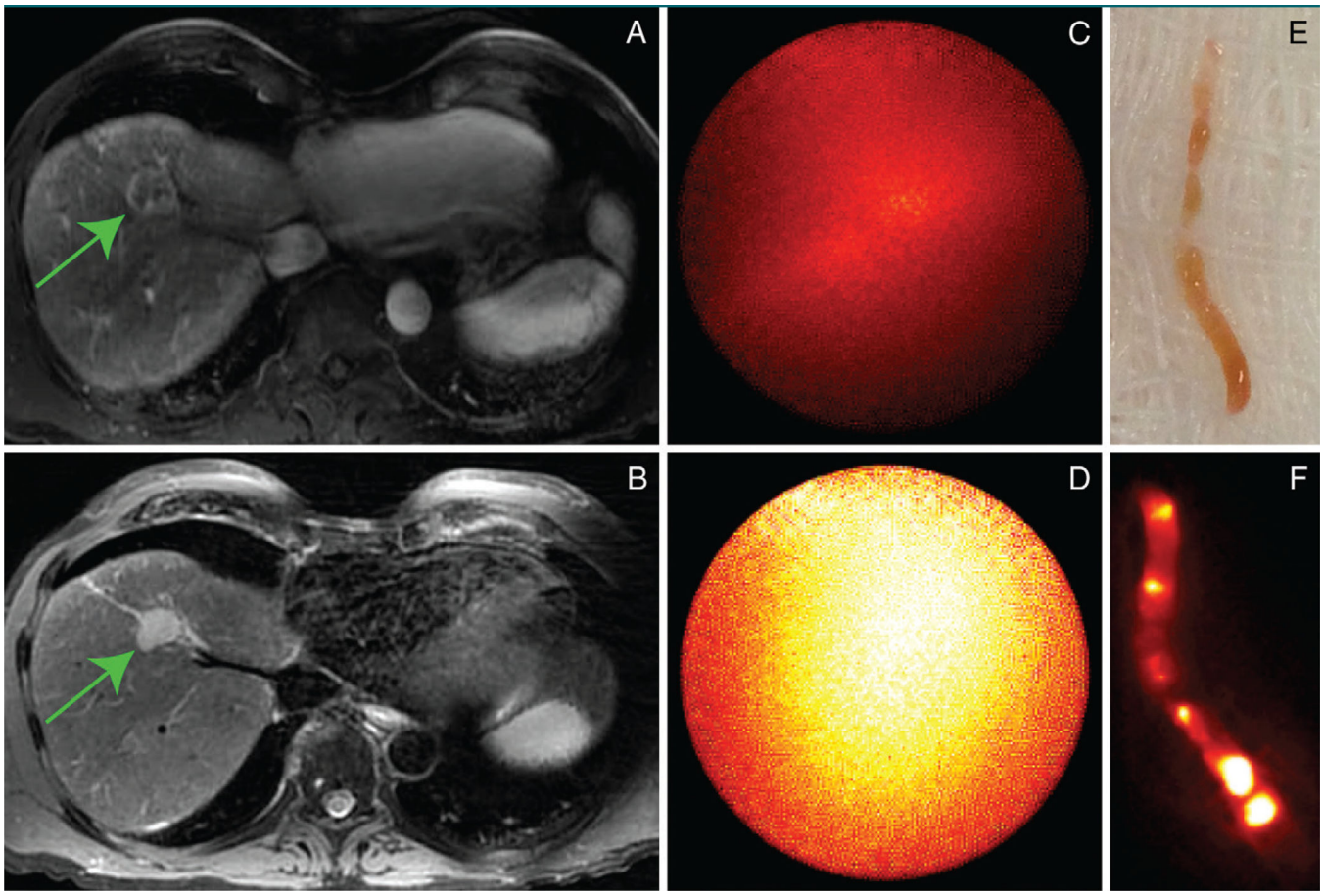

Figure 4.

Screening gadopentetate dimeglumine–enhanced MR images show, *A*, 21-mm enhancing lesion on a T1-weighted axial fat-suppressed image that demonstrates, *B*, intermediate-signal-intensity focal lesion (arrow) on a T2-weighted image in a 67-year-old man (patient 2) with HCV cirrhosis and prior history of renal cell carcinoma. Intraprocedural optical moIecular images demonstrate substantially increased ICG localization, *D*, in expected location of the lesion, *C*, relative to adjacent benign liver parenchyma during percutaneous biopsy. Surface reflectance imaging of, *E*, the core sample demonstrated, *F*, focal areas of increased ICG concentration. Final pathologic result was consistent with high-grade HCC.

Author Manuscript Author Manuscript Author Manuscript Author Manuscript

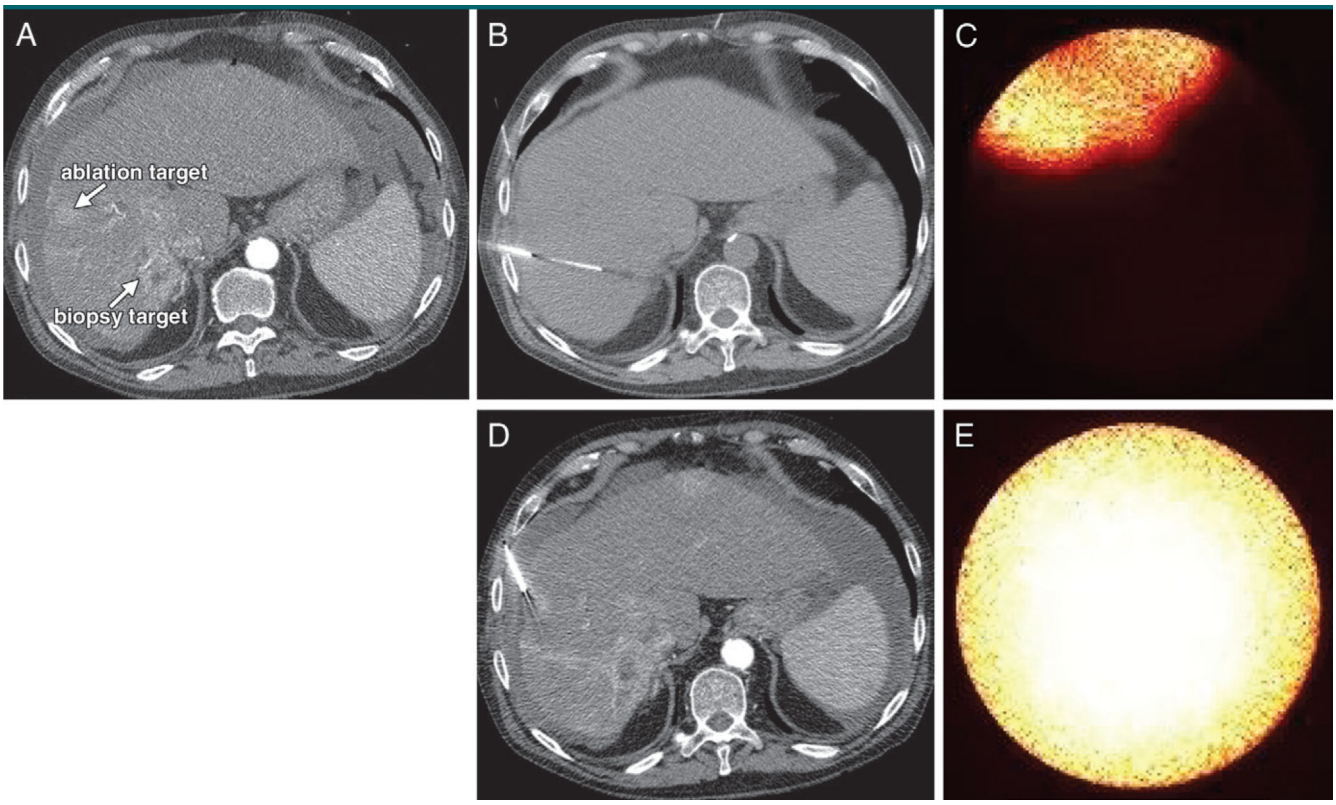

Figure 5.

A, CT scans in a 62-year-old man (patient 3) with HCV and alcoholic cirrhosis who underwent thermal ablation of an HCC in which biopsy was previously performed *(ablation target)*, as well as percutaneous biopsy of a second, centrally necrotic focal hepatic lesion *(biopsy target)* in a single procedure setting. Contrast-enhanced CT guidance was used for performance of, *B*, percutaneous biopsy and, *D*, thermal ablation; optical molecular images show that both, *C*, biopsy target and, *E*, ablation target demonstrate avid ICG enhancement. Pathologic results for the biopsy lesion were consistent with a high-grade necrotic HCC.

Author Manuscript Author Manuscript Author Manuscript Author Manuscript

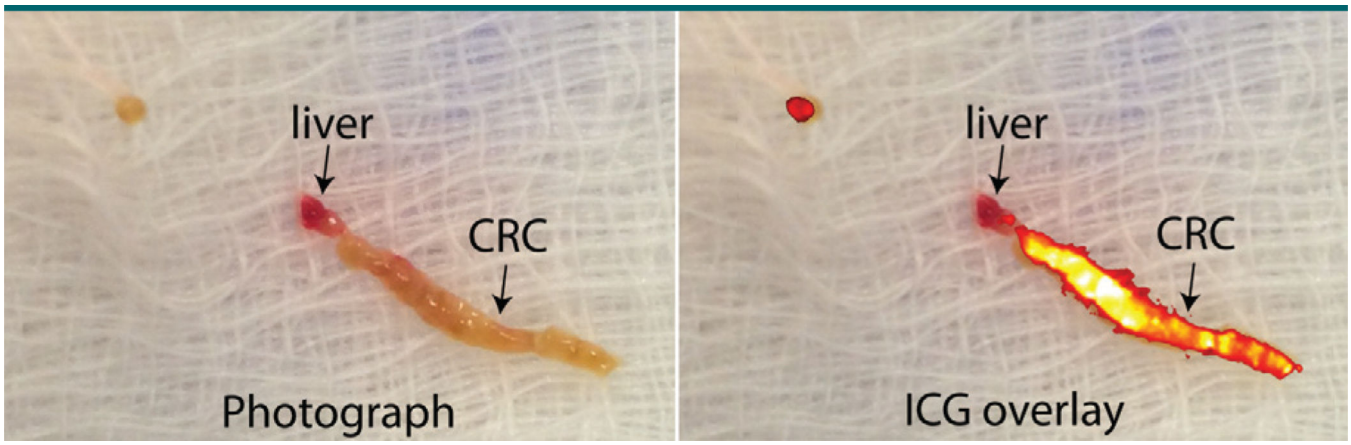

Figure 6.

Photograph and ICG overlay of core biopsy specimen from a 66-year-old man (patient 5) with a history of CRC. ICG overlay demonstrates intense fluorescence signal within the area of core sample that most likely corresponds to malignant tissue, while there is no appreciable fluorescence within the area that resembles adjacent normal liver. Pathologic result from the core specimen was consistent with metastatic CRC.

Author Manuscript Author Manuscript Author Manuscript Author Manuscript

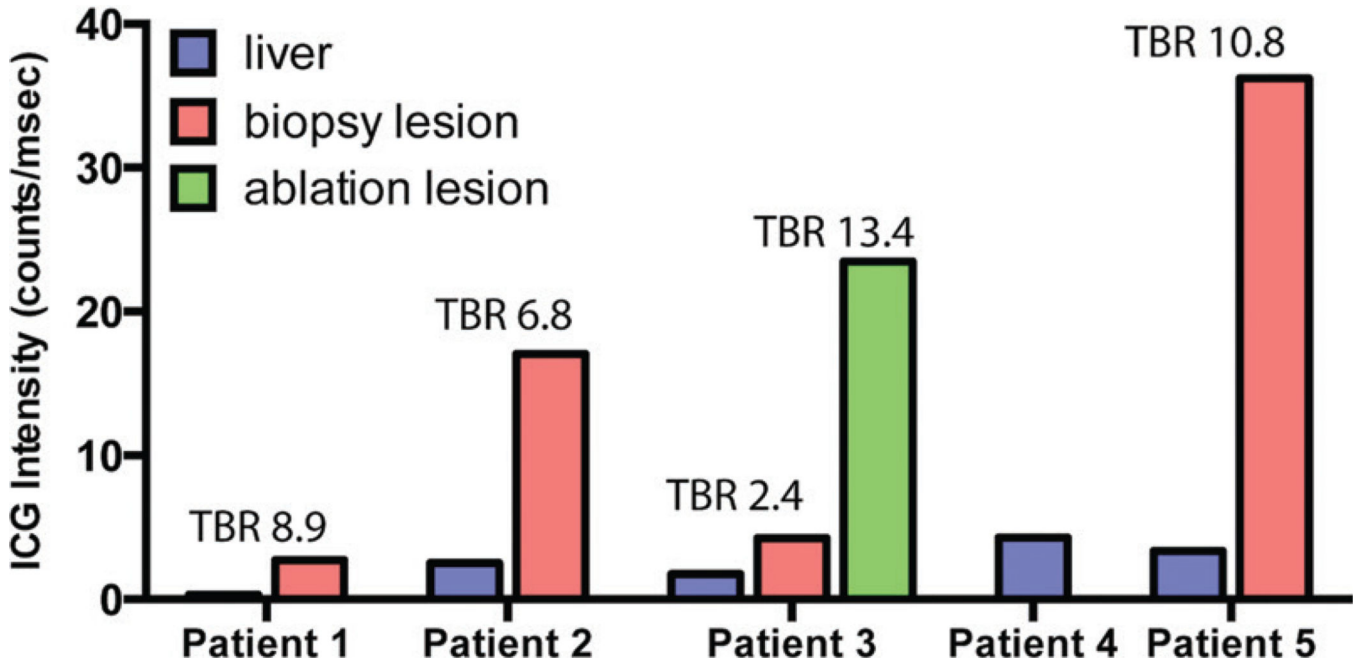

Figure 7.

Plot of normalized ICG fluorescence intensity measurements for background liver, biopsy lesions, and ablation targets for all five patients. While there is variability in the intensity of the background ICG signal, TBRs for all lesions were high (range, 2.4–13.4; median, 7.9).

Author Manuscript

Author Manuscript

Author Manuscript

Author Manuscript

Table 1

Point-of-Care Epifluorescence OMI System Properties

Property	Value
Dimensions (mm)*	250 × 200 × 70
Field of view (mm)	38 × 38
Working distance (mm)	140
Primary magnification	8.1×
Sensor resolution	
Spatial (pixels)	1388 × 1038
Temporal (frames/sec)	15
Bit depth	12

*Dimensions are width by height by depth.

Author Manuscript Author Manuscript Author Manuscript Author Manuscript

Table 2

Clinical Trial Participant Demographics

Patient No./Age(y)/Sex	Liver Disease	Prior Surgery	Prior Chemotherapy	Laboratory Values			Target Lesion Size (mm)
				Total Bilirubin (mg/dL)*	AST (U/L)†	ALT (U/L)†	
1/55/M	None	None	None	0.6	33	52	13
2/67/M	HCV cirrhosis, Child-Pugh class A5	None	None	0.4	175	249	21
3/62/M	HCV, alcoholic cirrhosis; Child-Pugh class A6	None	None	0.6	53	18	15, ablation
3/62/M	HCV, alcoholic cirrhosis; Child-Pugh class A6	None	None	0.6	53	18	18, biopsy
4/73/M	Hemochromatosis cirrhosis, Child-Pugh class A5	None	None	0.5	44	49	10
5/66/M	None	Partial colectomy	None	0.6	19	14	17

Note.—ALT = alanine aminotransferase, AST = aspartate aminotransferase, HCV = hepatitis C virus.

*To convert to Système International units in micromoles per liter, multiply by 17.104.

†To convert to Système International units in microkatals per liter, multiply by 0.0167.

Author Manuscript Author Manuscript Author Manuscript Author Manuscript

Table 3

Clinical Trial Procedure Summary

Patient No.	Procedure	Time from ICG Injection to Procedure (h)	Added Procedure Time (min)	Adverse Events	Procedure Imaging Modality	TBR	Final Pathologic Result
1	Biopsy	26	4	None	US	8.9	Granulomatous inflammation
2	Biopsy	23	2	None	US	6.8	HCC, high grade
3	Ablation	19.5	1	None	Contrast-enhanced CT	13.4	HCC, pseudoacinar type, grade 1
3	Biopsy	24	2	None	Contrast-enhanced CT	2.4	HCC with necrosis
4	Biopsy plus ablation	24	4	None	Contrast-enhanced CT	NA	Benign liver parenchyma with mild fatty liver disease
5	Biopsy	22	2	None	Nonenhanced CT	10.8	CRC metastasis

Note.—Contrast-enhanced = contrast material–enhanced

Radiology. Author manuscript; available in PMC 2016 March 01.